A NEW FUZZY MORPHOLOGY APPROACH BASED ON THE FUZZY-VALUED GENERALIZED DEMPSTER-SHAFER THEORY

SAFAR HATAMI, BABAK N. ARAABI, and CARO LUCAS

ABSTRACT. In this paper, a new Fuzzy Morphology (FM) based on the Generalized Dempster-Shafer Theory (GDST) is proposed. At first, in order to clarify the similarity of definitions between Mathematical Morphology (MM) and Dempster-Shafer Theory (DST), dilation and erosion morphological operations are studied from a different viewpoint. Then, based on this similarity, a FM based on the GDST is proposed. Unlike previous FM's, proposed FM does not need any threshold to obtain final eroded or dilated set/image. The dilation and erosion operations are carried out independently but complementarily. The GDST based FM results in various eroded and dilated images in consecutive α-cuts, making a nested set of convex images, where each dilated image at a larger α-cut is a subset of the dilated image at a smaller α-cut. Dual statement applies to eroded images.

1. Introduction

Since the MM has been introduced by Matheron and Serra in 1964 [1], significant developments have happened in both theoretical and practical aspects of MM. For the first time, MM is applied to image processing by Matheron [2] and Serra [1,3]. They deal with binary images as sets. As a result, the basic operations of MM are interpreted as basic filters on images, where translation of structuring element (SE) over an image and applying the essential operations of set theory such as union and intersection, turn into basic processing of binary images.

Gray-scale MM is a natural extension of binary MM. The MM is used in many computer vision applications such as noise suppression [4], feature extraction [4], edge detection [4,5], image filtering [6,7,8], skeleton representation and image edge enhancement [9]. One of the more celebrated fuzzy MM approaches is recently introduced by Sinha and Dougherty (SD) [10]. In fuzzy MM, images are not considered as crisp sets, but they are considered as fuzzy ones. In SD's approach, the set union and intersection operations are replaced with fuzzy bold union and intersection, respectively, to formulate fuzzy dilation and erosion.

This is not the only extension of MM to fuzzy sets, as other researchers proposed different extensions [11,12,13,14]. However, in this paper, we deal only with SD's FM, where the input image and SE are fuzzy [15,16], and erosion is defined on the basis of fuzzified set intersection, resulting a fuzzy image. This image is defuzzified by a threshold and one and only one nonfuzzy result will be obtained eventually. The dilated image is obtained from the eroded one, then.

Accepted:
Key words and phrases: Generalized Dempster-Shafer theory, Mathematical Morphology, Fuzzy Morphology, Generalized Dempster-Shafer Theory's Fuzzy Morphology

In this paper, using a fuzzy generalization of the DST, proposed by Lucas and Araabi (LA) [17], a novel approach to FM is introduced. In LA's GDST, belief (*bel*) and plausibility (*pls*) measures for a body of evidence with fuzzy focal elements, are defined as fuzzy numbers. They generalize the DST by assuming successive α-cuts of the focal elements, and a set-valued variant of fuzzy extension principle [18]. Applying the idea of belief and plausibility measures defined in LA's GDST to MM, results in some well-defined convex fuzzy eroded and dilated images.
Introduced GDST based FM is free from thresholds. Dilated and eroded images are obtained independently in GDST's FM. Besides, dilated and eroded image of $\alpha 1$-cut is a subset of a dilated and eroded image of $\alpha 2$-cut, where $\alpha 2 \le \alpha 1$ and $\alpha 1 \le \alpha 2$, respectively. It should be noted that Bloch and Maitre [19] have considered fuzzification of morphology operations in the context of α-cut being completely different from eroded and dilated image in α-cut.
This paper is organized as follows: Section 2 reviews Matheson's MM and SD's FM. Section 3 reviews DST and describes Yen's GDST as well as LA's GDST. In Section 4, we propose a correspondence between MM and DST at first and then use this correspondence to introduce a FM based on the LA's GDST. The main advantages of proposed FM are discussed as well. Finally, simulation results and conclusions are presented in Section 5 and Section 6, respectively.

2. Review of Mathematical Morphology and Fuzzy Morphology

2.1 Matheron's Mathematical Morphology

The two most important morphological operations are dilation and erosion. However, before there formal definition some more basic definition are in order [4].

Basic Definitions: Let A and B be sets in Z^2, with components $a=(a_1,a_2)$ and $b=(b_1,b_2)$, respectively. The set A is practically binary image and the set B is commonly referred to as the structuring element in morphological operations. The translation of A by $x=(x_1,x_2)$, denoted $(A)_x$, is defined as

$$(A)_x = \{c \mid c = a + x, \text{for } a \in A\} \tag{1}$$

The reflection of B, denoted $-B$, is defined as

$$-B = \{x \mid x = -b, \text{for } b \in A\} \tag{2}$$

The complement of set A is

$$A^c = \{x \mid x \notin A\} \tag{3}$$

Finally, the difference of two sets A and B, denoted $A - B$, is defined as

$$A - B = \{x \mid x \in A, x \notin B\} = A \cap B' \tag{4}$$

Dilation: With A and B as sets in Z^2 and $\varnothing$ denoting the empty set, the dilation of A by B, denoted $A \oplus B$, is defined as

$$A \oplus B = D(A,B) = \{x \mid (B)_x \cap A \neq \varnothing\} \tag{5}$$

Thus the dilation process consists of shifting B by x and then the dilation of A by B is the set of all x displacement such that B and A overlap by at least one nonzero element.

Erosion: For set A and B in Z^2, the erosion of A by B, denoted $A\Theta B$, is defined as

$$A\Theta B = \varepsilon(A,B) = \{x \mid (B)_x \subseteq A\} \tag{6}$$

that is, the erosion of A by B is the set of all points x such that B, translated by x, is contained in A.

2.2 Sinha and Dougherty's Fuzzy Morphology

As mentioned earlier, both image and SE are fuzzy set in the FM. Let us consider the erosion operation again. In the binary setting, a pixel x is part of the eroded image $A\Theta B$ if and only if the translation of SE B by amount x fits inside the image A. The SD's FM [15,16] revolves around the notion of *degree of fitness*. In the SD's FM, fuzzy erosion is defined via its membership function by $\mu_{\varepsilon(A,B)} = I(A,(B)_x) = \tau$ if and only if $(B)_x$ is a subset of A to the degree τ. In particular, an indicator for fuzzified set inclusion I is defined in such a way that $I(X,Y)$ measures belief in the proposition "X is a subset of Y", where X and Y as fuzzy sets. For example, it is proposed that

$$I(X,Y) = \inf_{z \in u} \min[1, \lambda(\mu_X(z) + \lambda(1 - \mu_Y(z)))] \tag{7}$$

where λ is a function that must satisfy a number of constraints and u is domain of fuzzy binary image. Dilation (D) is then defined by duality

$$D(A,B) = \varepsilon(A^c, -B)^c \tag{8}$$

Example 2.1. Consider the following image A and SE B

$$A = \begin{pmatrix} 0.2 & 1.0 & 0.8 & 0.1 \\ 0.3 & 0.9 & 0.9 & 0.2 \\ 0.1 & 0.9 & 1.0 & 0.3 \end{pmatrix} \tag{9}$$

$$B = \begin{pmatrix} 0.8 & 0.9 \end{pmatrix} \tag{10}$$

A few eroded images are shown in Table 1.

Table 1- The SD's FM based eroded image using λ_n, where $n \in \{1, 1.25, 1.5, 2, 10, 15\}$.

$n = 1$	$n = 1.25$	$n = 1.5$
$\begin{pmatrix} 0.20 & 0.40 & 0.90 & 0.20 \\ 0.20 & 0.50 & 1.00 & 0.30 \\ 0.20 & 0.30 & 1.00 & 0.40 \end{pmatrix}$	$\begin{pmatrix} 0.24 & 0.49 & 0.99 & 0.25 \\ 0.24 & 0.60 & 1.00 & 0.37 \\ 0.24 & 0.37 & 1.00 & 0.48 \end{pmatrix}$	$\begin{pmatrix} 0.28 & 0.57 & 1.00 & 0.29 \\ 0.28 & 0.70 & 1.00 & 0.43 \\ 0.28 & 0.43 & 1.00 & 0.56 \end{pmatrix}$
$n = 2$	$n = 10$	$n = 15$
$\begin{pmatrix} 0.36 & 0.72 & 1.00 & 0.38 \\ 0.36 & 0.87 & 1.00 & 0.55 \\ 0.36 & 0.55 & 1.00 & 0.70 \end{pmatrix}$	$\begin{pmatrix} 0.89 & 1.00 & 1.00 & 1.00 \\ 0.89 & 1.00 & 1.00 & 1.00 \\ 0.89 & 1.00 & 1.00 & 1.00 \end{pmatrix}$	$\begin{pmatrix} 0.96 & 1.00 & 1.00 & 1.00 \\ 0.96 & 1.00 & 1.00 & 1.00 \\ 0.96 & 1.00 & 1.00 & 1.00 \end{pmatrix}$

Suppose $n \le 2$. If we threshold the eroded image at 0.9, then we obtain

$$X = \begin{pmatrix} 1 \\ 1 \\ 1 \end{pmatrix} \tag{11}$$

We have a nonfuzzy eroded image (11), which is obtained through thresholding. We should obtain dilated image from eroded image in SD's FM. In addition, after defuzzification (thresholding) one and only one eroded image is obtained.

3. Dempster-Shafer Theory and Its Generalizations

Before proposing GDST based FM, we review DST as well as GDST's that are established by LA and Yen.

3.1. Dempster-Shafer Theory

The DST could be considered as generalization of probability theory. Consider a set-valued mapping $\Gamma: X \to P_\Omega$, where P_Ω is the set of all nonfuzzy subsets of Ω, and the referential set Ω is a finite set. Assume a probability measure ρ over X. Now, what can be said about a probability measure over Ω that is induced by Γ? Dempster shows that for each $B \subset \Omega$, $P(B)$ belongs to the following interval [20]

$$P(B) \in \left[\rho_l(B), \rho_h(B)\right] = \left[\sum_{j: A_j \subset B} m_j, \sum_{j: A_j \cap B \neq \phi} m_j\right] \tag{12}$$

in which $A_j \in P_\Omega$ is any nonempty member of the range of Γ and

$$m_j = \left(\frac{\rho\left(\Gamma^{-1}\left(A_j\right)\right)}{1-\rho\left(\Gamma^{-1}\left(\ \right)\right)} \right) \quad \forall\, A_j \in \text{Range}(\Gamma) \tag{13}$$

About ten years later Shafer introduced his evidence theory and defined *bel* and *pls* functions [21]. Consider a referential set $\Omega = \{\omega_1, \omega_2, \omega_3, ..., \omega_n\}$; a body of evidence is defined as follows

$$\begin{gathered} \{A_1, A_2, ..., A_l\}\ \{m_1, m_2, ..., m_l\} \\ \varnothing \neq A_j \subset \Omega \quad m_j > 0 \quad \sum m_j = 1 \end{gathered} \tag{14}$$

in which each A_j is a focal element, and m_j is the corresponding mass value. Evidence theory could be considered as a direct generalization of Bayesian statistics. One may think of mass values as probability density values; but in evidence theory, mass values are assigned to the subsets of Ω instead of the elements of Ω; therefore, it conveys a higher level of uncertainty and is capable of modeling both ignorance and indeterminism. Shafer defined the concepts of belief and plausibility as two measures over the subsets of Ω in an axiomatic manner and then he showed that *bel* and *pls* with following definitions

$$bel : P_\Omega \to [0,1] \quad bel(B) = \sum_{j:A_j \subset B} m_j \quad \forall B \in P_\Omega \tag{15}$$

$$pls : P_\Omega \to [0,1] \quad pls(B) = \sum_{j:A_j \cap B \neq \varnothing} m_j \quad \forall B \in P_\Omega \tag{16}$$

were actually identical to upper and lower bounds of probability as defined by Dempster (12). When we refer to DST we mean both approaches with their corresponding results and interpretation.

Example 3.1. Consider a body of evidence in the DST over $\Omega = \{\omega_1, \omega_2, ..., \omega_{15}\}$ with focal elements

$$\begin{aligned} A_1 &= \{\omega_1, \omega_2, \omega_3, \omega_4\} \\ A_2 &= \{\omega_3, \omega_4, \omega_5, \omega_6\} \\ A_3 &= \{\omega_{11}, \omega_{12}\} \\ A_4 &= \{\omega_4, \omega_7, \omega_8, \omega_9, \omega_{10}\} \\ A_5 &= \{\omega_{13}, \omega_{14}, \omega_{15}\} \end{aligned} \tag{17}$$

We calculate *bel* and *pls* of $B = \{\omega_1, \omega_2, \omega_3, \omega_4, \omega_5, \omega_6, \omega_7, \omega_8, \omega_{11}, \omega_{12}\}$, where $m_1 = 0.1$, $m_2 = 0.2$, $m_3 = 0.25$, $m_4 = 0.15$, and $m_5 = 0.3$

(18) $$bel(B) = m_1 + m_2 + m_3 = 0.55$$

(19) $$pls(B) = m_1 + m_2 + m_3 + m_4 = 0.7$$

Figure 1 shows schematic of Example 2.1, in which A_1, A_2, and A_3 are subsets of B, and A_4 intersects B. Hence, *bel* and *pls* of *B* are calculated in (18) and (19).

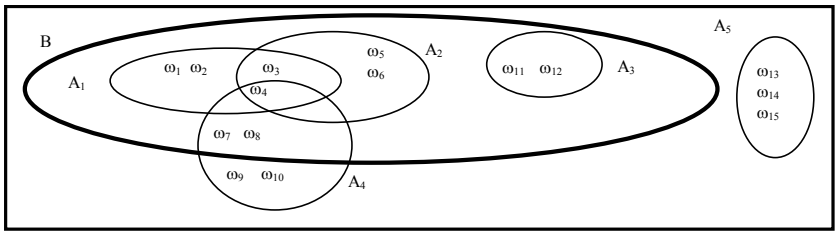

Figure 1- Schematic of example 2.1.

3.2. Generalized Dempster-Shafer Theory

While DST assigns mass values to the subsets, rather than the elements of Ω, one may still wish to build up the probability concept over the fuzzy subsets of Ω. Let us define a fuzzy body of evidence like (14), the only difference being that all A_j's, and B, can be normal fuzzy subsets of Ω as well as nonfuzzy ones.

Yen's generalization says

(20) $$bel(B) = \sum_j m_j \sum_k (\alpha_k - \alpha_{k-1}) \times \inf_i \max\{1 - \mu_{A_{j\alpha_k}}(\omega_i), \mu_B(\omega_i)\}$$

(21) $$pls(B) = \sum_j m_j \sum_k (\alpha_k - \alpha_{k-1}) \times \sup_i \min\{\mu_{A_{j\alpha_k}}(\omega_i), \mu_B(\omega_i)\}$$

where $A_{j\alpha_k} = \{\omega_i | \mu_{A_j}(\omega_i) \geq \alpha_k\}$.

Example 3.2. Consider body evidence in the DST over $\Omega = \{0,1,2,3,4,5,6,7,8,9\}$ with focal elements

(22) $$A = \{0.25/1, 0.5/2, 0.75/3, 1/4, 1/5, 0.75/6, 0.5/7, 0.25/8\}$$

(23) $$C = \{0.5/5, 1/6, 0.8/7, 0.4/8\}$$

We want to compute *bel*(*B*) and *pls*(*B*) where

(24) $$B = \{0.5/2, 1/3, 1/4, 1/5, 0.9/6, 0.6/7, 0.3/8\}$$

According to Yen's generalization, we replace A and C with A and C's α-cuts and then distribute their mass values among α-cuts.

$$
\begin{array}{ll}
A_{0.25} = \{1,\ 2,\ 3,\ 4,\ 5,\ 6,\ 7,\ 8\} & m(A_{0.25}) = 0.25m(A) \\
A_{0.5} = \{2,\ 3,\ 4,\ 5,\ 6,\ 7\} & m(A_{0.5}) = 0.25m(A) \\
A_{0.75} = \{2,\ 3,\ 4,\ 5,\ 6,\ 7\} & m(A_{0.75}) = 0.25m(A) \\
A_{1} = \{\ 4,\ 5\} & m(A_{1}) = 0.25m(A) \\
C_{0.4} = \{5,\ 6,\ 7{,}8\} & m(C_{0.4}) = 0.4m(C) \\
C_{0.5} = \{5,\ 6,\ 7\} & m(C_{0.5}) = 0.1m(C) \\
C_{0.8} = \{6,\ 7\} & m(C_{0.8}) = 0.3m(C) \\
C_{1} = \{6\} & m(C_{1}) = 0.2m(C)
\end{array} \tag{25}
$$

Thus, instead of initial body of evidence including A and C along with their mass values, we consider body of evidence in (25) with eight focal elements. If we compute the belief and plausibility using (20) and (21) we obtain the following results

$$bel(B) = 0.6m(A) + 0.54m(C) \tag{26}$$

$$pls(B) = m(A) + 0.95m(C) \tag{27}$$

where $m(A) = 0.2$ and $m(C) = 0.8$.

In contrast to the Yen's generalization, in the LA's generalization [17], each focal set is replaced with its α-cuts, and mass value of focal element is assigned to each α-cut [18]. Now, (20), (21) are utilized to obtain *bel* and *pls*. For example, considering body of evidence in (22) and (23), *pls* and *bel* of B in (24), are computed in accordance with the LA's generalization, and shown in Figure 2. Table 2 provides some details of this computation.

Table 2- Consecutive α-cuts of body of evidence

α	A_α	C_α	$m(A_\alpha)$	$m(C_\alpha)$
0.25	{1,2,3,4,5,6,7,8}	{5,6,7,8}	$m(A)$	$m(C)$
0.40	{2,3,4,6,7}	{5,6,7,8}	$m(A)$	$m(C)$
0.50	{2,3,4,6,7}	{5,6,7}	$m(A)$	$m(C)$
0.75	{3,4,6,7}	{6,7}	$m(A)$	$m(C)$
0.80	{4,5}	{6,7}	$m(A)$	$m(C)$
1.00	{4,5}	{6}	$m(A)$	$m(C)$

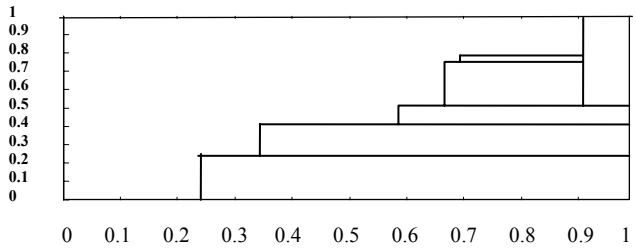

Figure 2- Probability of *B* based on LA's generalization, Y-axis: α-cut, X-axis: probability.

4. Proposed Fuzzy Morphology

4.1. Correspondences between Mathematical Morphology and DST

We want to consider the similarities of relations between morphology and Dempster-Shafer theory. There are correspondences between plausibility and belief concepts in DST, with dilation and erosion concepts in morphology, respectively. For example, let us consider image A that we want to dilate and erode by SE B. At first, our objective is to compute the number of pixels of the first row in eroded and dilated image. The locations of translated SE B over the first row of image A are shown in Figure 3(a).

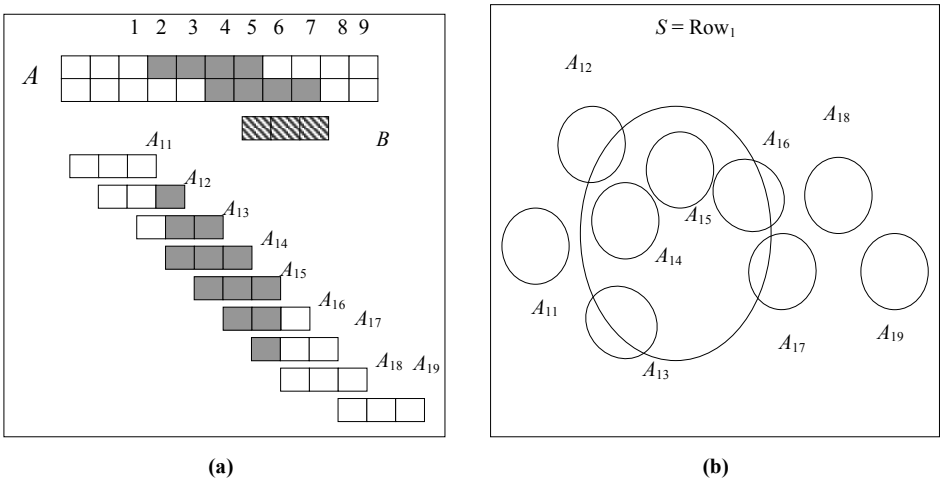

Figure 3- (a) Image *A* and SE *B* and the location of translated SE *B* over the first row of image *A*. (b) Erosion and dilation of first row in image *A* and SE *B* regarding DST interpretation.

Now we construct a body of evidence for A_{ij} 's in Figure 3(a), as shown in Figure 3(b), where for every A_{ij} we let $m_{ij} = 1$ (mass values are not normalized). Plausibility and belief of the first row are

(28) $$bel = m_{14} + m_{15}$$

(29) $$pls = m_{12} + m_{13} + m_{14} + m_{15} + m_{16} + m_{17}$$

In fact, computed *pls* and *bel* are the numbers of pixels in the first row of dilated and eroded images. This procedure can be done for next rows. This claim can be proved as follows (Row number = *j*)

(30) $$bel_j(A) = \sum_{i:A_{ij} \subset \text{Rowj}} m_{ij} = \left| \left\{ x_j \mid (B)_{x_j} \subset A \right\} \right| = \left| A \Theta B_{x_j} \right|$$

(31) $$pls_j(A) = \sum_{i:A_{ij} \cap \text{Rowj} \neq \varnothing} m_{ij} = \left| \left\{ x_j \mid (B)_{x_j} \cap A \neq \varnothing \right\} \right| = \left| A \oplus B_{x_j} \right|$$

where $x = (x_1, x_2)$ and $x_j = (j, x_2)$.

In the next step, we put the computed number of pixels from aforementioned procedure around the central point of the row to construct the dilated and eroded images. Note that:

A) Indeed, this algorithm is applied with this SE to all images having a central point in each row.
B) For every arbitrary SE, we should perform the first step for all pixels, and then put them around the central point in each row and column. If we obtain the intersection of these two images in horizontal and vertical directions, we reach eroded and dilated image based on Matheron's method.
C) If one row or column has several centers; we should apply this algorithm around each center.

Proposed algorithm: The DST based Mathematical nonfuzzy Morphology Algorithm can be summarized as follows:

1) Extract the focal element for each column or row.
2) Form the body of evidence for each column or row of image.
3) Assign mass value $m = 1$ to all focal elements.
4) Draw *S* corresponding to each row or column as Figure 3(b).
5) Calculate *bel* and *pls* as number of pixels of eroded and dilated image in each row or column.

4.2. Generalized Dempster-Shafer Theory's Fuzzy Morphology

Consider the fuzzy image A and fuzzy SE B in Figure 4(a). To erode and dilate image A, we move B over A. According to the DST based Morphology Algorithm, Section 4.1, the set A' is the body of evidence, and B' is the set including all of translated B's, as S in Section 4.1 - B' and A' are shown in Figure 4(a). The *bel* and *pls* of B' are equivalent to erosion and dilation, respectively.

GDST's FM algorithm for computation of dilated and eroded image is as follows:

We move the SE B over image A, therefore, it results a set A_{ij} with dimension B corresponding to SE. Now, the plausibility and belief can be computed in accordance with DST based Morphology Algorithm in Section 4.1. It means that we obtain K intervals for *pls* and *bel* corresponding to each pixel where K is the number of α-cuts for each A_i. In the next step, we sum all intervals related to pixels of a row and column in horizontal and vertical directions, respectively, for a special α-cut. Indeed, we have K intervals for each pixel. This process is shown in Figure 4(b).

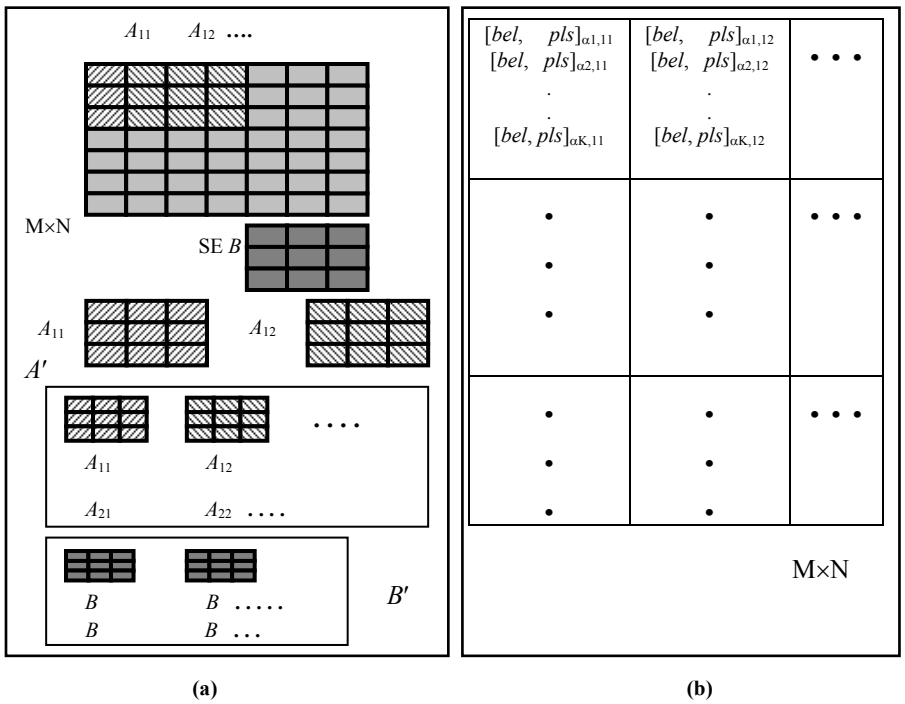

Figure 4- (a) Fuzzy image A and SE B and body of evidence A' and S= B'. (b) K intervals for each pixel, where [*bel*,*pls*]αk,ij is the interval for α-cut at k, i = number of row, and j = number of column.

Now, *pls* and *bel* in horizontal and vertical directions are computed as follows

$$\text{Row}_i(\alpha_k) = \left[\sum_{j=0}^{N-1} bel_{\alpha k,ij}, \sum_{j=0}^{N-1} pls_{\alpha k,ij} \right] = \left[bel_{ri}(k), pls_{ri}(k) \right] \tag{32}$$

$$\text{Col}_i(\alpha_k) = \left[\sum_{j=0}^{M-1} bel_{\alpha k,ij}, \sum_{j=0}^{M-1} pls_{\alpha k,ij} \right] = \left[bel_{ci}(k), pls_{ci}(k) \right] \tag{33}$$

Hence, $bel_{ri}(k)$ and $pls_{ri}(k)$ is the number of pixels of eroded and dilated image in horizontal direction in *i*-th row with α-cut at *k*, and $bel_{ci}(k)$ and $pls_{ci}(k)$ is the number of pixels of eroded and dilated image in vertical direction in *j*-th row with α-cut at *k*, respectively.

4.3. GDST's Fuzzy Morphology Advantageous

Proposed approach does not need any threshold. At the end of this algorism, we have some dilated and eroded images in different α-cuts. In this method, dilated and eroded images are obtained independently. If B is convex, and each chosen block A_i of image with dimension B is convex too, different interval α-cuts are proved to be convex [17]. This is true when the α-cut for α = 1 is not null. In this case, summation of intervals at each row or column for each α is convex. In case that α-cut for α = 1 is null, one may replace the intervals corresponding to α-max instead of intervals with α > α-max. This claim may be proved as follows:

For *j*-th row, consider intervals $\left[bel, pls \right]_{\alpha k,ij}$ $i = 1,...,M$, and assume

$$\forall i \in \{1,...,M\} \text{ and } \alpha k_1 < \alpha k_2 \ \left[bel, pls \right]_{\alpha k_1,ij} \subseteq \left[bel, pls \right]_{\alpha k_2,ij} \tag{34}$$

As a result,

$$\therefore \left[\sum_{j=0}^{N-1} bel_{\alpha k,ij}, \sum_{j=0}^{N-1} pls_{\alpha k,ij} \right]_{\alpha k1,i} \subseteq \left[\sum_{j=0}^{N-1} bel_{\alpha k,ij}, \sum_{j=0}^{N-1} pls_{\alpha k,ij} \right]_{\alpha k2,i} \tag{35}$$

5. Simulation Results

Consider A and B in (9) and (10), respectively. The Figure 5(a) presents the *bel* for different α-cuts and Figure 5(b) presents the *pls* for different α-cuts. As shown in Figure 5, six eroded and dilated image are gained.

Eroded image in smaller α-cut is subset of eroded image in larger α-cut. Similarly, dilated image in larger α-cut is subset of dilated image in smaller α-cut. For example, consider that eroded image in α-cut at 0.1 is subset of eroded image in α-cut at 0.2,

while dilated image in α-cut at 0.2 is subset of dilated image in α-cut at 0.1. This definition for dilation and erosion does not demand for any threshold. Proposed FM forms dilated and eroded image separately. In comparison with SD's FM, the later method results in one eroded image using thresholding, and then dilated image is derived through utilizing the eroded image.

Figure 5- (a) *bel* of *A* and *B* in (9) and (10) that is equivalent with eroded image in consecutive α-cuts (b) *pls* of *A* and *B* in (9) and (10) that is equivalent with dilated image in consecutive α-cuts.

6. Conclusion

In this paper, a novel approach to FM base on the GDST was proposed. Similarities between DST and MM were exploited to build a FM concept over a fuzzy-valued generalization of the DST. In this method, in accordance to each α-cut of the body of evidence, one dilated image and one eroded image were obtained, independently. The eroded image at α_1-cut is a subset of eroded image at α_2-cut, and the dilated image at α_2-cut is a subset of dilated image at α_1-cut, where $\alpha_1<\alpha_2$. As a result, eroded and dilated images were happened to be convex fuzzy sets, while definition of morphological operations did not demand for any user-defined threshold. In a follow up research, we are trying to apply our proposed method to few case studies, which helps us to better compare GDST's FM with SD's FM, in practice.

REFERENCES

[1] J. Serra, *Image analysis and mathematical morphology*, Academic press, London, UK, (1982).
[2] G. Matheron, *Random sets and integral geometry*, John Wiley, New York, USA, (1975).
[3] J. Serra, *Introduction to mathematical morphology*, Computer Vision, Graphics and Image Processing, **35(3)** (1986) 283-305.
[4] R. C. Gonzalez and R. E. Woods, *Digital image processing*, Prentice Hall, New York, USA, (2002).
[5] J. S. J. Lee, R. M. Haralick, and L. G. Shapiro, *Morphologic edge detection*, IEEE Transactions on Robotics and Automation, **3(2)** (1987) 142-156.
[6] P. Maragos and R. W. Schafer, *Morphological filters-Part I: Their set-theoretic analysis and relations to linear shift-invariant filter*s, IEEE Transactions on Acoustics, Speech, and Signal Processing, **35(8)** (1987) 1153-1169.
[7] P. Maragos and R. W. Schafer, *Morphological filters-Part II: Their relations to median, order-statistics, and stack filters*, IEEE Transactions on Acoustics, Speech, and Signal Processing, **35(8)** (1987) 1170-1184.

[8] R. L. Stevenson and G. R. Arce, *Morphological filters: Statistics and further syntactic properties*, IEEE Transactions on Circuits and Systems, **34(11)** (1987) 1292-1305.
[9] L. XiangJi and D. RunTao, *Fuzzy morphological operators to edge enhancing of images*, Proc. 4th IEEE Int. Conf. Signal Processing, Beijing, China, **2** (1998) 1017-1020.
[10] D. Sinha and E. R. Dougherty, *Fuzzy mathematical morphology*, Visual Communication and Image Representation, **3(3)** (1992) 286-302.
[11] I. Bloch and H. Maitre, *Fuzzy mathematical morphologies: A comparative study*, Pattern Recognition, **28(9)** (1995) 1341-1387.
[12] C. R. Giardina and D. Sinha, *Image processing using pointed fuzzy sets*, Proc. VIII SPIE Conf. Intelligent Robots and Computer Vision: Algorithms and Techniques, Philadelphia, USA, **1192** (1989) 659-668.
[13] V.Goetcherian, *From binary to gray tone image processing using fuzzy logic concepts*, Pattern Recognition, **12(1)** (1980) 7-15.
[14] M. Kauffman and M. M. Gupta, *Fuzzy mathematical models in engineering and management science*, Elsevier, North-Holland, New York, USA (1988).
[15] D. Sinha and E. R. Dougherty, *A General axiomatic theory of intrinsically fuzzy mathematical morphologies*, IEEE Transactions on Fuzzy Systems, **3(4)** (1995) 389-403.
[16] D. Sinha, P. Sinha, E. R. Dougherty, and S. Batman, *Design and analysis of fuzzy morphological algorithms for image processing*, IEEE Transactions on Fuzzy Systems, **5(4)** (1997) 570-584.
[17] C. Lucas and B. N. Araabi, *Generalization of the Dempster-Shafer theory: A fuzzy-valued measure*, IEEE Transactions on Fuzzy Systems, **7(3)** (1999) 255-270.
[18] B. N. Araabi, N. Kehtarnavaz, and C. Lucas, *Restrictions imposed by the fuzzy extension of relations and functions*, Journal of Intelligent and Fuzzy Systems, **11(1/2)** (2001) 9-22.
[19] I. Bloch and H. Maitre, *Mathematical morphology on fuzzy sets*, Proc. Int. Workshop Mathematical Morphology and its Applications to Signal Processing, Barcelona, Spain, (1993) 151-156.
[20] A. P. Dempster, *Upper and lower probabilities induced by a multi-valued mapping*, Annals of Mathematical Statistics, **38(2)** (1967) 325-339.
[21] G. Shafer, *A mathematical theory of evidence*, Princeton University Press, Princeton, USA, (1976).

Abbreviations:

FM: Fuzzy Morphology
GDST: Generalized Dempster-Shafer Theory
MM: Mathematical Morphology
DST: Dempster-Shafer Theory
SD: Sinha and Dougherty
LA: Lucas and Araabi
SE: Structuring Element
bel: Belief
pls: Plausibility

SAFAR HATAMI, RESEARCH ASSISTANT, CONTROL AND INTELLIGENT PROCESSING CENTER OF EXCELLENCE, ELECTRICAL AND COMPUTER ENGINEERING DEPARTMENT, UNIVERSITY OF TEHRAN, P.O. BOX 14395/515, TEHRAN, IRAN.
E-mail address: **s.hatami@ece.ut.ac.ir**

BABAK N. ARAABI *, ASSISTANT PROF., CONTROL AND INTELLIGENT PROCESSING CENTER OF EXCELLENCE, ELECTRICAL AND COMPUTER ENGINEERING DEPARTMENT, UNIVERSITY OF TEHRAN, P.O. BOX 14395/515, TEHRAN, IRAN.
E-mail address: **araabi@ut.ac.ir**

CARO LUCAS, PROF., CONTROL AND INTELLIGENT PROCESSING CENTER OF EXCELLENCE, ELECTRICAL AND COMPUTER ENGINEERING DEPARTMENT, UNIVERSITY OF TEHRAN,
P.O. BOX 14395/515, TEHRAN, IRAN.
E-mail address: **lucas@ipm.ir**

* CORRESPONDING AUTHOR